NAVORD REPORT 3064

NEEDLE STATIC-PRESSURE PROBES INSENSITIVE TO FLOW INCLINATION IN SUPERSONIC AIR STREAMS

15 MARCH 1954

Aeroballistic Research Report 231

NEEDLE STATIC-PRESSURE PROBES INSENSITIVE TO FLOW INCLINATION IN SUPERSONIC AIR STREAMS

Prepared by:

L. W. Walter and E. J. Redman

ABSTRACT: Tests were made to develop small static pressure needle-probes insensitive to flow inclination in a two-dimensional supersonic flow. A probe configuration was obtained which could be used to measure static pressure within ±2% at angles of attack from -8° to +16° at Mach number 1.5 and from -4° to +12° at Mach number 2.5. Assuming that the flow can be resolved into independent axial and transverse components, agreement between the pressure variation predicted using data taken with cylinders transverse to the flow and the pressure variation versus angle of attack measured with the probes was obtained.

This report contains information of importance to workers who must measure static pressures in supersonic air streams. The experimental data were obtained during December 1953, January 1954, and February 1954 in the 12 x 12 cm Aerophysics Wind Tunnel No. 6 and the 18 x 18 cm Aerophysics Wind Tunnel No. 3 at the U. S. Naval Ordnance Laboratory. This work was sponsored by the Office of Naval Research under Task Number NR-31 (54).

The authors wish to acknowledge the work contributed by R. Bransom in constructing the static pressure probes.

EDWARD L. WOOLYARD
Captain, USN
Commander

H. H. KURZWEG, Chief
Aeroballistic Research Department
By direction

CONTENTS

	Page
Introduction.	1
Test Procedure.	2
Results and Discussion.	3
Comparison with Theory.	5
Reynolds Number Effects	6
Effect of Axial Location of Pressure Orifices . . .	6
Effect of Orifice Size and Alignment.	7
Conclusions	7
References.	8
Appendix A.	9

ILLUSTRATIONS

Figure 1. Sketch of Long and Short Needle Probes
Figure 2. Long Probe Mounted in the 12 x 12 cm Tunnel
Figure 3. Pressure Error vs. Angle of Attack of Probe
Figure 4. Pressure Error vs. Angle of Attack of Probe
Figure 5. Pressure Error vs. Angle of Attack of Probe
Figure 6. Pressure Error vs. Angle of Attack of Probe
Figure 7. Angle of Attack Range of Probes for Given Error Limit at Various M
Figure 8. Comparison of Pressure Distributions with Empirical Theory
Figure 9. Comparison of Pressure Distributions with Empirical Theory
Figure 10. Comparison of Pressure Distributions with Empirical Theory
Figure 11. Comparison of Pressure Distributions with Empirical Theory
Figure 12. Theoretical Pressure Distributions for $\theta = 40°$ Probes at Various M
Figure 13. Pressure at $\alpha = 0°$ vs. Axial Location of Orifice

Table I. Dimensions of the Four Probes Tested
Table II. Ratio of static pressures measured by the [illegible]

SYMBOLS

α angle of attack of the probe axis, degrees; measured in the plane of symmetry of the orifices (see Figure 1)

θ angle of offset of a point on the probe from the plane of symmetry of the orifices, degrees (see Figure 1)

ϕ angle between the probe axis and the tangent to the probe surface which intersects the axis, degrees

M Mach number of the free-stream

M_c Mach number of the flow component normal to the probe axis

P free-stream static pressure

P_m static pressure on the probe surface

q free-stream dynamic pressure

C_p pressure coefficient, $\frac{P_m - P}{q}$

NEEDLE STATIC-PRESSURE PROBES INSENSITIVE TO FLOW INCLINATION IN SUPERSONIC AIR STREAMS

INTRODUCTION

1. During the course of an investigation of the wake behind a circular cylinder it became necessary to measure static pressures. This task was complicated by the inclination of the air flow and by the small width of the viscous wake of the cylinder (a ½" diameter cylinder was used). A static probe was required that would be small enough so that it produced little disturbance of the flow. It must also be insensitive to flow inclinations for at least moderate angles of inclination, say angles up to 10° or 15°.

2. Several methods for measuring both static pressure and flow inclination exist. These methods suffer from several disadvantages; the mechanism is usually intricate, the data reduction is relatively complicated, and the pressure sensing element is, in general, large. It is the last of these disadvantages that led us to try some modification of the conventional static pressure needle probe that would be insensitive to flow inclination. The needle probe can be made almost as small as one desires. To this end we have combined the ideas of several authors.

3. The work of Jones (reference a) and Allen and Perkins (reference b) has shown that the flow about slender axially symmetric bodies inclined to the air stream can be considered quite simply. If the angle of inclination is not too large, the flow can be resolved into two independent streams; one perpendicular to the axis of the body and the other parallel to it. An expression for the pressure coefficient, $C_p = (P_m - P)/q$, at any point on the body can then be obtained in closed form if incompressible potential flow is assumed. The pressure coefficient is given as a function of the angle of attack, α, the azimuthal angle θ (measured from the angle of attack plane) and the axial distance, x (see Appendix A). This expression shows that for every axial position, there is a θ for which C_p is zero independent of the angle of attack. An orifice located at this position should then measure the true static pressure for all angles of attack.

4. Cooper and Hamilton (reference c) have shown that this is actually the case for a parabolic body of revolution at Mach number 1.6 if the angle of attack is not too large. They suggested that static needle probes insensitive to angle of

attack could also be built by properly choosing the angular position of the orifice with respect to the angle of attack plane.

5. However, in the Mach number range in which the probes are to be used, the cross flow Mach number, $M_c = M \sin \alpha$, reaches values of 0.8 for the higher angles of attack. Therefore, it is unrealistic to assume incompressible potential cross flow; the effect of compressibility becomes important for flow about a cylinder when the Mach number is higher than 0.3. Any comparison with theory must use a viscous, compressible theory for the transverse flow component. Unfortunately no such theory exists for the flow about a cylinder.

6. A considerable amount of experimental information on the pressure distributions on cylinders in cross flow, however, does exist. If the assumption that the flow can be resolved into two independent components is valid, then the pressure distribution about a cylinder inclined to a flow with Mach number, M, should be identical with the experimental pressure distribution about a cylinder in a cross flow with Mach number M_c. The pressure as a function of α for a fixed value of θ and the free-stream Mach number can be obtained from the experimental cylinder distributions in this way.

7. Several cone-cylinder probes have been tested. Two orifice locations, $\theta = 33°$ and $\theta = 52°$, were used. The empirical method described above predicted that an orifice location of $\theta = 33°$ would be relatively insensitive to angle of attack for $M = 2.5$; unpublished NOL data on ogive-cylinders suggested relative insensitivity to angle of attack for Mach numbers approaching 3 if an orifice location $\theta = 52°$ were used. The results of tests using these orifice locations are described below.

TEST PROCEDURE

8. The tests to be described were carried out in the 12 x 12 cm and 18 x 18 cm NOL supersonic wind tunnels. Both these tunnels are blow-down tunnels which can be operated continuously. They operate with atmospheric supply temperature and pressure for Mach numbers from 1.6 to 5.0. A detailed description of both tunnels is given in reference 4.

9. Each probe consisted of a steel or copper tube, 0.050" in diameter, tipped with a cone 8 tube diameters long (7° vertex angle). Two holes were drilled radially in the cylindrical portion of the probe. Table I shows the orifice size, angular

separation of the orifices, and distance of the orifices from the cone tip for the four probes which were tested. Sketches of the probes are shown in Figure 1.

Probe Designation	Angular Separation of Orifices (2θ)	Orifice Size	Distance of Orifice from Cone Tip
33° short	66°	.008"	10 diameters
52° short	104°	.013"	10 diameters
33° long	66°	.008"	35 diameters
52° long	104°	.013"	35 diameters

Table I. Features of the Four Probes Tested

10. The probes were "telescoped" through "O" rings into a holder which was rigidly attached to a circular insert. The insert was mounted in the tunnel side wall replacing one of the glass windows. The length of the probe was adjusted so that the orifices fell on the axis of rotation of the mounted insert; thus the orifices remained at the same point in the flow for all angles of attack. The angle θ was set by placing the orifices so that the angle of attack plane bisected the line joining them; the angle of attack of the probe was varied by turning the insert through a given angle with respect to the tunnel axis.

11. There are two possible errors in the angular measurements with the probe in the wind tunnel; the error in setting θ and the error in the angle of attack caused by bending of the probe. The error in setting θ is almost wholly removed by having two pressure orifices. This is discussed in paragraph 23. The error introduced by the probe bending at high angles of attack was checked using a transit sighted on the probe through a glass window in the tunnel side wall. A comparison of the actual angle of attack as measured by the transit with that for which the probe was set shows a difference of 1° in the worst case -- probes having copper shanks; the steel-shanked probes showed negligible bending. Corrections for bending have been applied in cases where necessary.

RESULTS AND DISCUSSION

12. The ratios of the measured static pressures, P_m, to the static pressure, P, measured at zero angle of attack are plotted in Figures 3 through 6 as functions of the angle of attack, α.

Table II gives the measured- to supply- pressure ratios at zero angle of attack for the probes tested. The static pressure measured with the long probe has here been assumed to be the correct free-stream static pressure. The table shows that the short probes give pressures which are slightly low. This is not a serious defect since a small correction can be applied to the measured pressures. The correction which was empirically determined for the short probes is given below.

$(P_m/P_) = .0149 - .0046M$ (here M can be the Mach number corresponding to the measured value of the static pressure)

Nominal Mach number	1.5	2.5	2.9	3.2
P_m/P_o (long probe)	.253	.0604	.0329	.0187
P_m/P_c (short probe)	.246	.0582	.0306	.0185

Ratio of static pressures measured by the probes at zero angle of attack to the supply pressure for the Mach numbers used.

Table II

13. If an error of 1 percent or 2 percent is permissible in the static pressure measurement, then the curves show that either the short or the long probe with hole separations, $2\theta = 66°$, can be used in the range M = 1.5 through M = 2.5 for a relatively wide range of positive α. At M = 1.5 both probes read the static pressure to within 2 percent for α up to +16°. At M = 2.9, the maximum permissible α has decreased to 5°. The short probe with a hole separation $2\theta = 104°$, however, gives the static pressure to within 2 percent for α up to +11° for M = 2.9. Figure 7 shows the angle of attack range of each probe for a given percentage deviation (1 percent to 2 percent) from the pressure at $\alpha = 0$.

14. It is apparent from the above curves that neither value for the hole separation, 2θ, works for all the Mach numbers. For $\theta = 33°$, the long probe is relatively insensitive to angle of attack in the low and intermediate Mach number range; the short probe with $\theta = 52°$ is relatively insensitive to angle of attack for Mach numbers between 2.9 and 3.3.

15. The pressure as a function of angle of attack is unsymmetric with respect to positive and negative values of α. Thus, the probes cannot be improved by drilling two more holes 180° from

the original holes. This can be seen by averaging the measured pressures for two values of α that differ in sign only. Such a procedure would decrease considerably the range of positive α for which the probe is good without materially increasing the negative range of α. This also means that a rough idea of the flow direction is necessary before these probes can be used with complete confidence.

Comparison with Theory

16. We have used the experimental pressure distributions about cylinders of Gowen and Perkins (reference e) to obtain pressure vs. angle of attack curves for the angles $\theta = 30°$, $33°$ and $52°$ using the method described in the introduction. These curves together with our experimental points are shown in Figures 8 through 11 for both long and short probes at $M = 1.57$ and $M = 2.92$. The curves for the remaining Mach numbers are similar. The $\theta = 30°$ curve in the figures shows the difference between the curves obtained from the experimental values of reference e and $P_m/P = 1$, the value predicted by potential theory for $\theta = 30°$.

17. The agreement between the pressure distributions for the long probes and the distributions derived from the data of Gowen and Perkins is quite good (see Figures 9 and 11). The largest deviation occurs at $M = 2.9$ for negative α. A turbulent cross flow boundary layer could be the cause of this disagreement. The NACA data used in plotting the curves were for a laminar boundary layer about a cylinder. For positive α and for θ less than $75°$, the pressure as a function of θ is nearly the same for either laminar or turbulent boundary layer. Since to our knowledge there exist no pressure distributions at the required Mach numbers for turbulent boundary layer about the cylinder, it was not possible to compare this case with the probe pressure distributions for negative α, i.e., for $\theta \geq 75°$.

18. We have also compared the pressure distributions for the short probes with the empirical method described above. Figures 8 and 10 show the results of this comparison. The agreement is not nearly so good as for the long probes. This, however, must be expected. A cylinder of finite length inclined to the flow direction bears some resemblance to a cylinder started impulsively from rest in a direction perpendicular to its axis. The development of the cross flow about the inclined cylinder as a function of axial distance is roughly comparable with the development of the flow as a function of time of a cylinder started impulsively from rest (references b and f). For

large axial distances or for long times the cross flow will have its steady state character; the "transients" will have disappeared. The short probe results are, therefore, not strictly comparable with the steady state NACA cylinder data since the cross flow presumably has not had time to assume its steady state character.

19. The agreement of the experimental results with the empirical theory can be used to obtain an estimate of the static pressure as a function of angle of attack for probes with any given value for θ. Figure 12, for example, shows the predicted variation of pressure with α for $\theta = 40°$. This probe configuration appears to be somewhat superior to that for which $\theta = 33°$ if 2 percent error in static pressure is permissible. The latter, however, gives the pressure within 1 percent for a wider range of α. Because of the large orifice size (with respect to probe diameter) on the experimental needle-probes, we do not think that a probe with dimensions similar to those used here but with $\theta = 40°$ would, in practice, give any greater insensitivity to angle of attack (see paragraphs 22 and 23 below).

Reynolds Number Effects

20. In the comparisons described above, the Reynolds numbers of the probes and those of the cylinders in cross flow were very different. The method can, nonetheless, be used because the pressure distribution about cylinders is little affected by Reynolds number variation if the boundary layer on the cylinder is laminar; the only parameter affecting the pressure distribution is the Mach number*. If the Reynolds number is high enough so that transition to a turbulent boundary layer occurs, the surface pressure distribution with the turbulent boundary layer is very different from the laminar case. However, transition occurs only for $\theta \geq 75°$ and thus only the negative values of α are affected.

Effect of Axial Location of Pressure Orifices

21. We have also measured the static pressure on the probe surface as a function of axial distance from the shoulder for $\alpha = 0$. The results of these measurements are shown in Figure 13. The curves show that, if the orifices are located 10 diameters from the shoulder, the pressure obtained will be the true static pressure for the Mach number range. This agrees with the results of Holder et al. (reference 6) who performed similar tests using ogival-nosed probes.

*It is assumed here that the Reynolds number is large enough so that the concept of a boundary layer is meaningful.

Effect of Orifice Size and Alignment

22. The pressure orifices are large in relation to the needle probe diameter; the two sizes used (.008" and .013" diameter) correspond to 18° and 30° of arc. Thus, the pressures obtained are averages over these arcs. However, this pressure will be the pressure that corresponds to a given θ if the pressure distribution is linear in the region covered by the orifice. This is very nearly so on cylinders in cross flow in the region $\theta = 20°$ to $\theta = 60°$. On this basis, the hole size is not important as long as it does not enter the nonlinear regions or cause local flow disturbances.

23. The linearity mentioned above and the use of two symmetrically placed orifices should remove errors due to small misalignments in setting the angle θ when the probe is placed in the tunnel. If the angle θ, as set, is a little in error, then one of the orifices has as much positive error of misalignment as the other has negative. These two errors should average out if the arcs subtended by the orifices remain in the linear part of the pressure distribution.

CONCLUSIONS

24. Cone cylinder needle probes have been built which give the free-stream static pressure within 2 percent for angles of attack up to plus 16° for Mach number 1.5 and for angles of attack up to plus 12° for Mach number 2.5 when the angle of yaw is zero.

25. The flow about such probes can be treated by resolving the flow velocity into an axial and transverse component and treating the two components as independent.

26. The effect of Reynolds number is negligible except for negative angles of attack (provided that the boundary layer approximation is applicable).

27. An orifice location equal to 10 diameters from the shoulder proved sufficient to insure complete pressure recovery with a cone length of 8 diameters and for Mach numbers $1.5 \leq M \leq 2.9$.

References

a. Jones, R. T., Effects of Sweep-back on Boundary Layer and Separation, NACA Report No. 884, 1947.

b. Allen, H. J., and Perkins, E. W., A Study of Effect of Viscosity on Flow over Slender Inclined Bodies of Revolution, NACA Report No. 1048, 1951

c. Cooper, M., and Hamilton, C. V., Orientation of Orifices on Bodies of Revolution for Determination of Stream Static Pressure at Supersonic Speeds, NACA TN No. 2592. 1952.

d. Lightfoot, J. R., The Naval Ordnance Laboratory Aeroballistic Research Facility, Naval Ordnance Laboratory Report (NOLR) No. 1079, 1950.

e. Gowen, F. E., and Perkins, E. W., Drag of Circular Cylinders for a Wide Range of Reynolds Numbers and Mach Numbers, NACA TN No. 2960, 1953.

f. Schwabe, M., Pressure Distribution in Nonuniform Two-Dimensional Flow, NACA TN No. 1039, 1943. (Translation of: Über Druckermittlung in der nichstationaren ebenen Stromung, Ingenieur-Archiv, Volume VI, No. 1, Feb 1935, pp. 34-50).

g. Holder, D. W., North, R. J., Chinneck, A., Experiments with Static Tubes in a Supersonic Air Stream, Parts I and II, ARC Report R&M No. 2782, Jul 1950.

APPENDIX A

1. Allen and Perkins show that if the body is "slender enough," i.e., if the longitudinal velocity component is very nearly equal in magnitude to the free-stream velocity, the pressure coefficient for any point on the body surface is given by:

$$C_p = 2 \tan\beta \sin\theta \sin 2\alpha + (1 - 4 \sin^2\theta) \sin^2\alpha + C_p\Big|_{\alpha=0} \quad \text{(A1)}$$

where α is the angle between the air stream and the axis of symmetry of the body, θ is the angular distance of a point on the body out of the plane in which α is measured, β is the angle formed by the intersection of the tangent to the body at the point in question with the axis of symmetry, and C_p is the pressure coefficient $\frac{P_M - P}{q}$

2. If the first two terms on the right-hand side of equation (A1) are set equal to zero, a relation between α and θ results for which C_p equals the pressure coefficient at zero angle of attack, $C_p\Big|_{\alpha=0}$

3. The angle θ that satisfies this condition for all α is 30°. To other values of θ for which $C_p = C_p\Big|_{\alpha=0}$, there correspond two and only two values of α for a given angle β.

4. Let us consider a needle probe which is a slender cone-cylinder. With the pressure orifice located on the cylindrical portion of the body $\tan\beta = 0$, so that the first term on the right side of equation (A1) is zero. Thus, if the orifice is located 30° out of the angle of attack plane ($\theta = 30°$) we find $C_p = C_p\Big|_{\alpha=0}$ for all α; i.e., the probe is insensitive to angle of attack. This prediction is true as long as the physical flow field is approximately potential flow and the probe is slender.

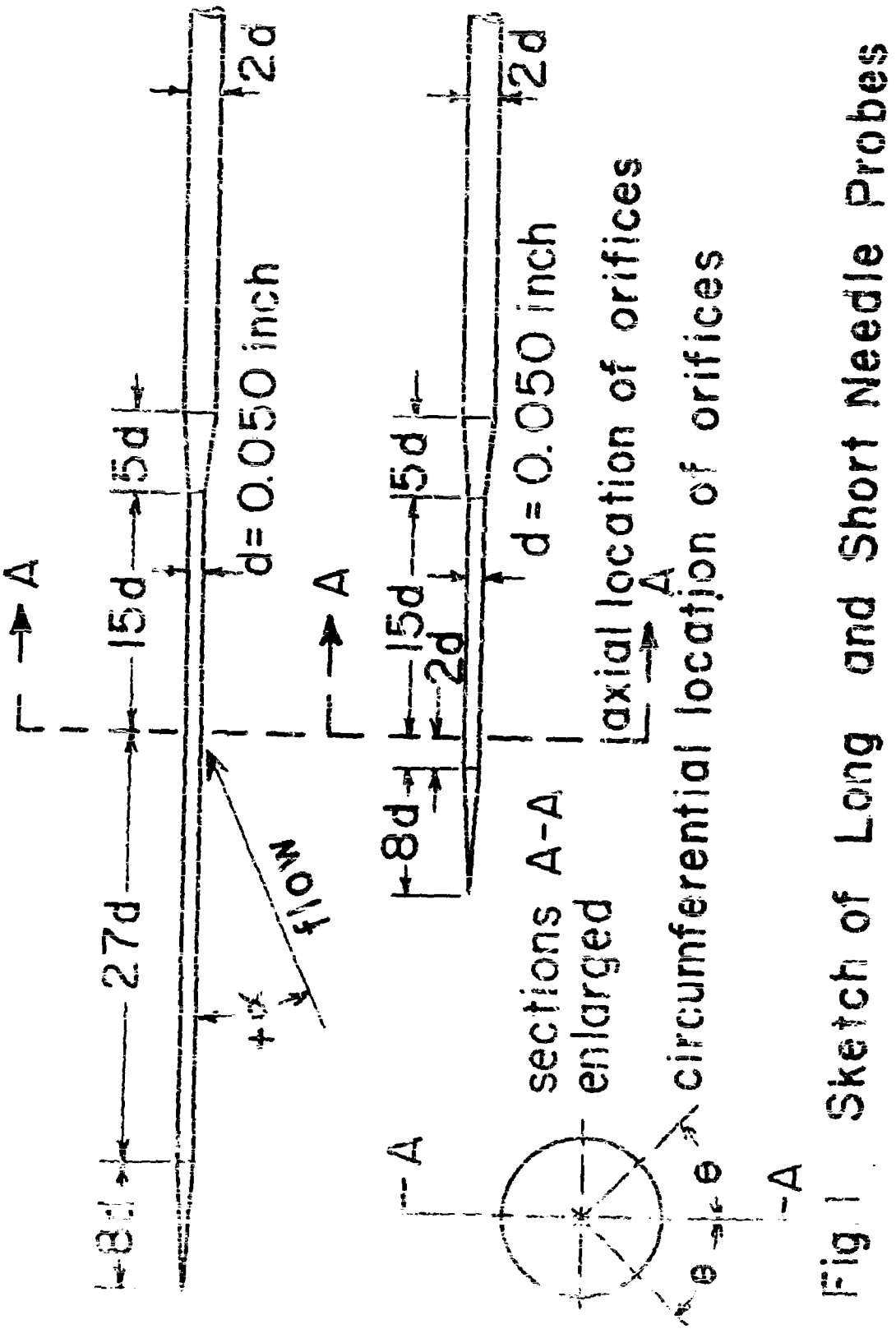

Fig 1 Sketch of Long and Short Needle Probes

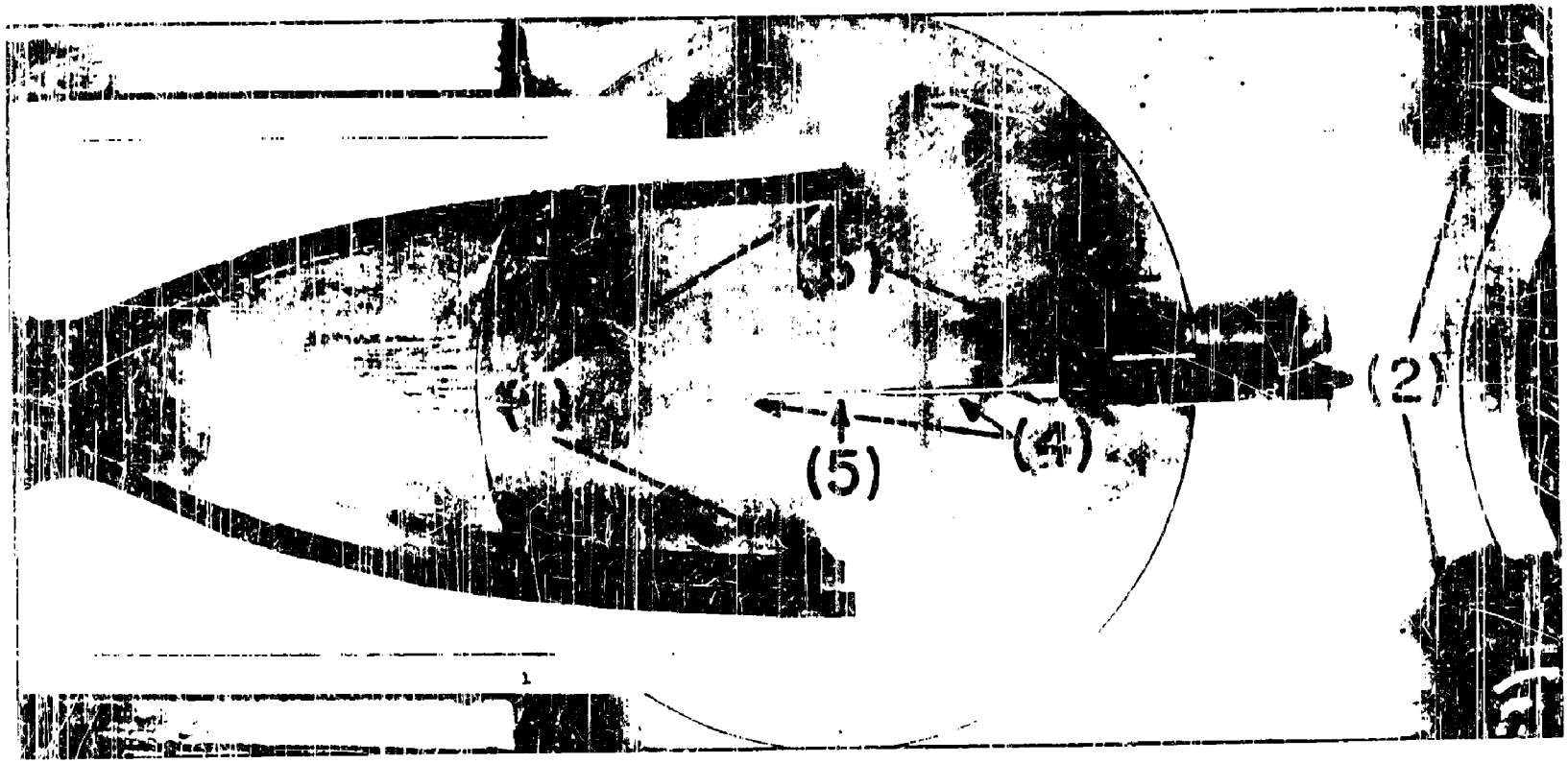

1) nozzle exit
2) diffusor entrance
3) insert
4) probe
5) orifices
6) holder

Fig. 2 Long Probe Mounted in the 12- x 12-Cm. Tunnel

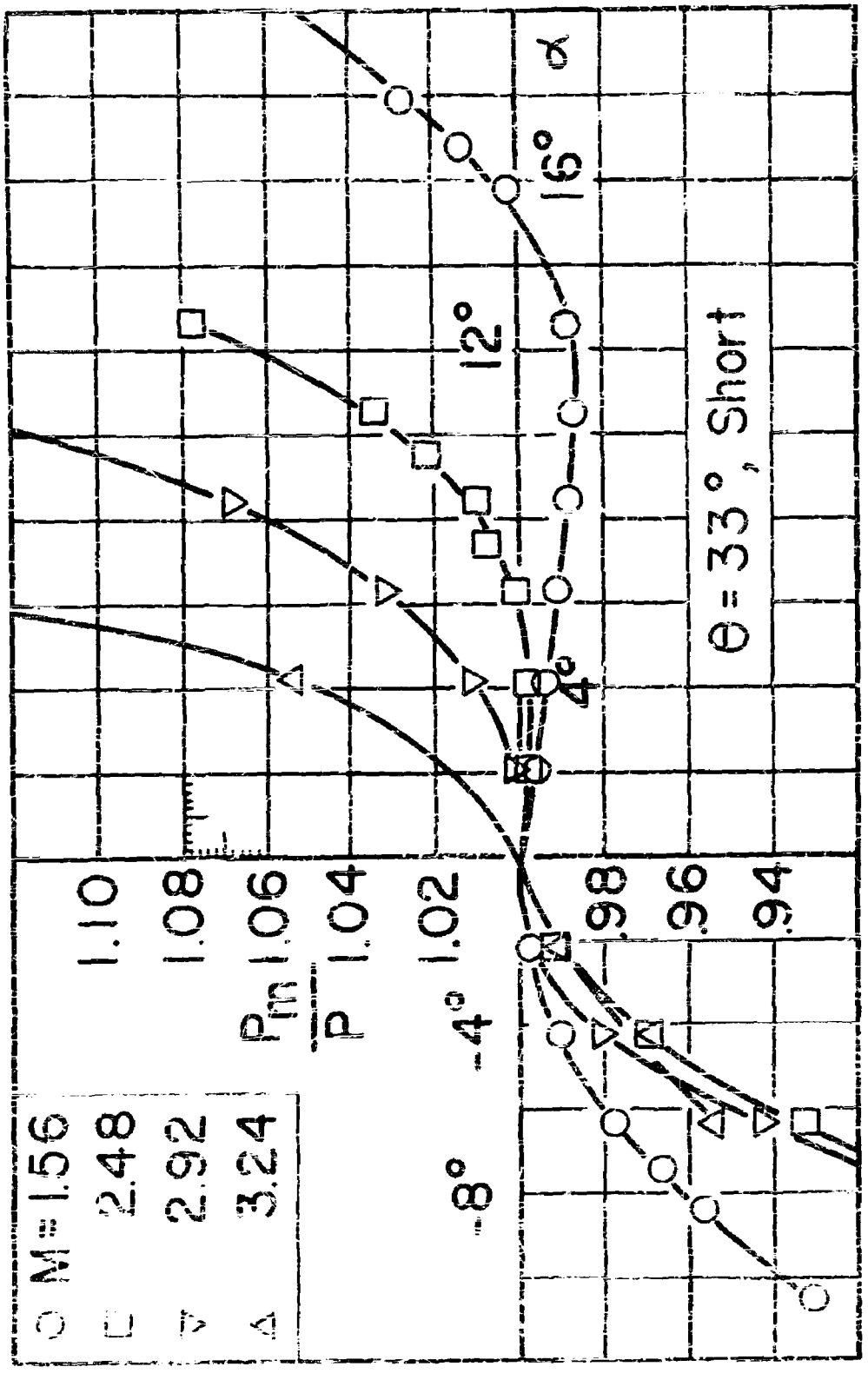

Fig. 3 Pressure Error vs Angle of Attack of Probe

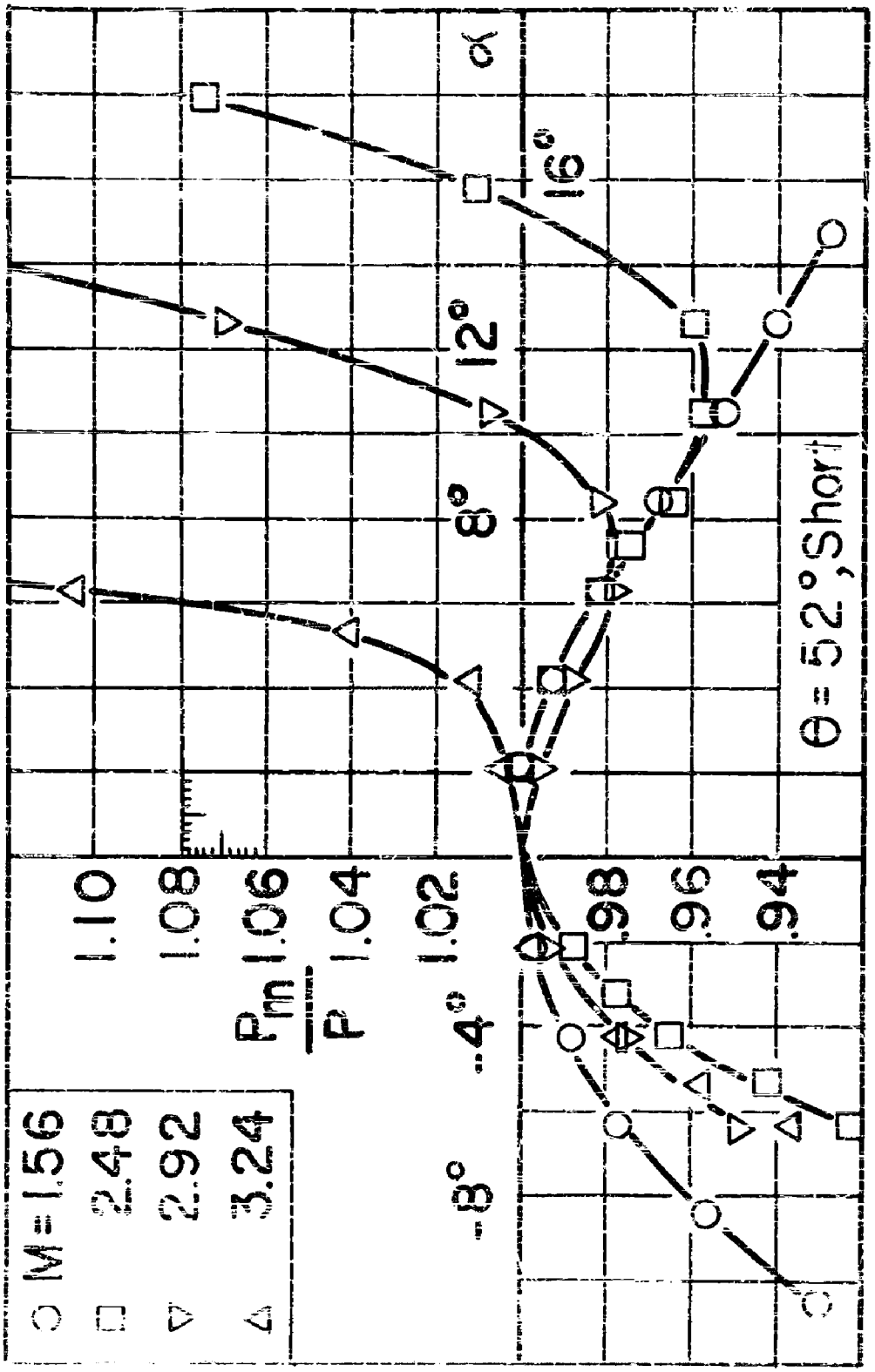

Fig. 4 Pressure Error vs Angle of Attack of Probe

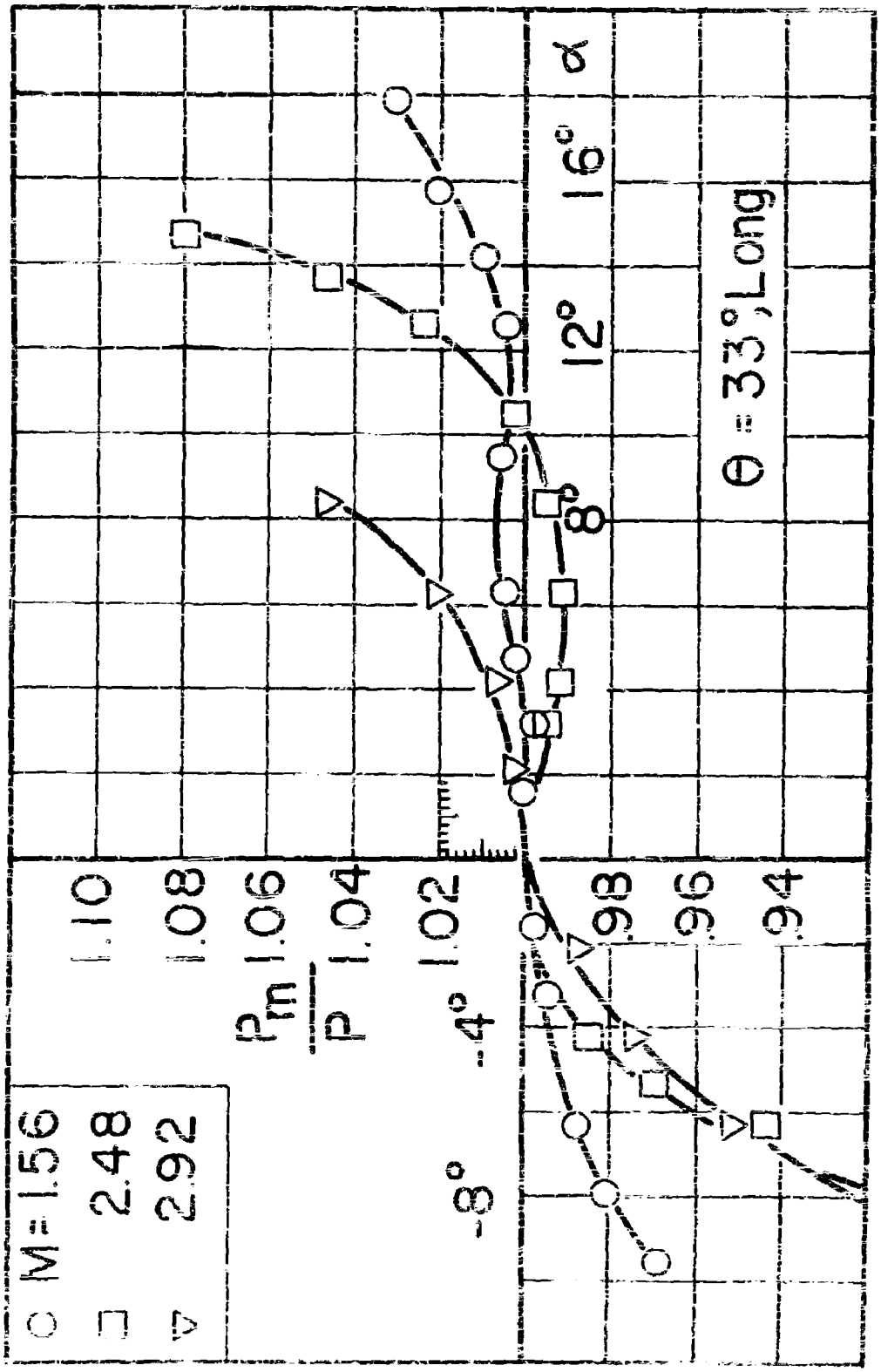

Fig. 5 Pressure Error vs Angle of Attack of Probe

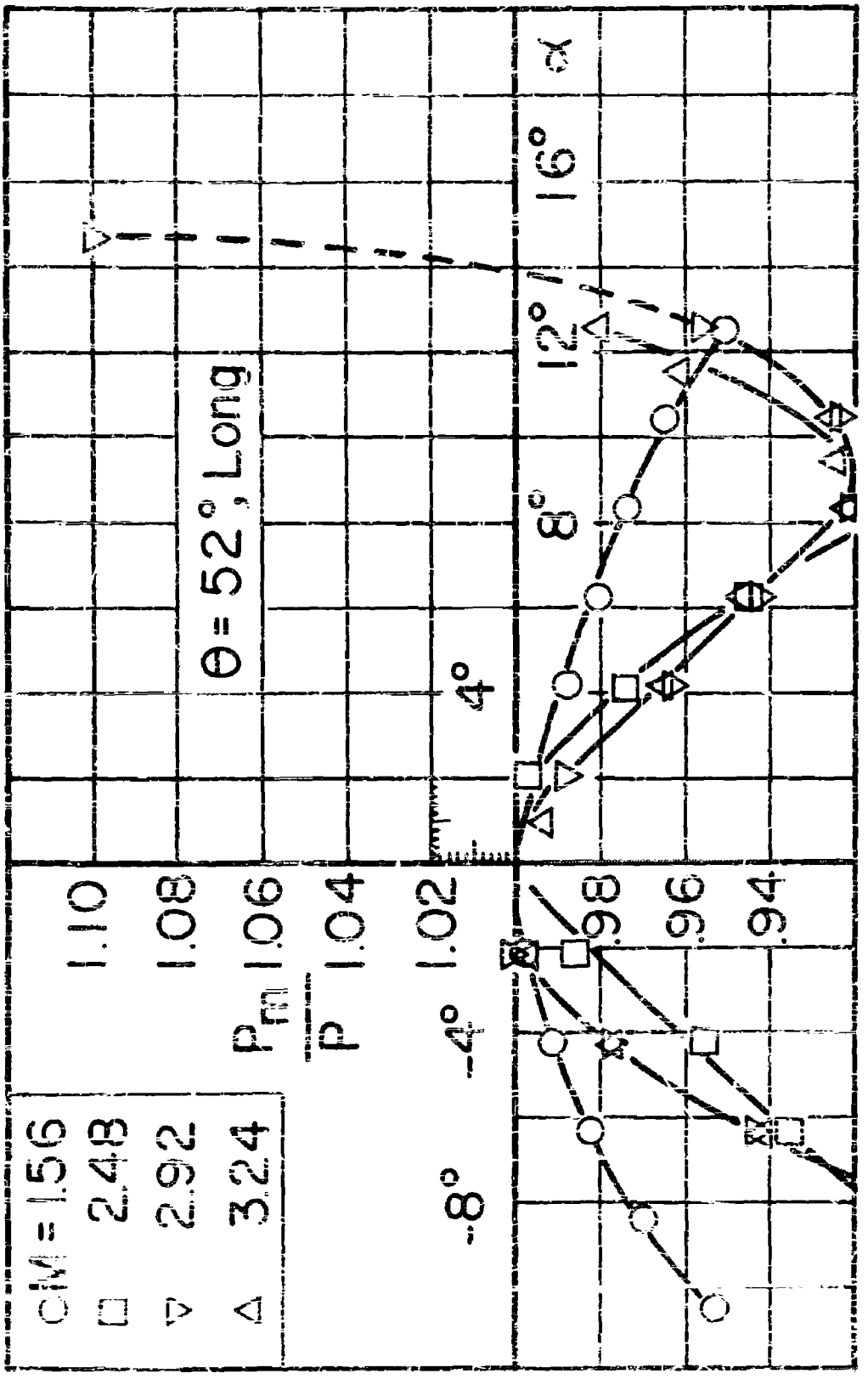

Fig. 6 Pressure Error vs Angle of Attack of Probe

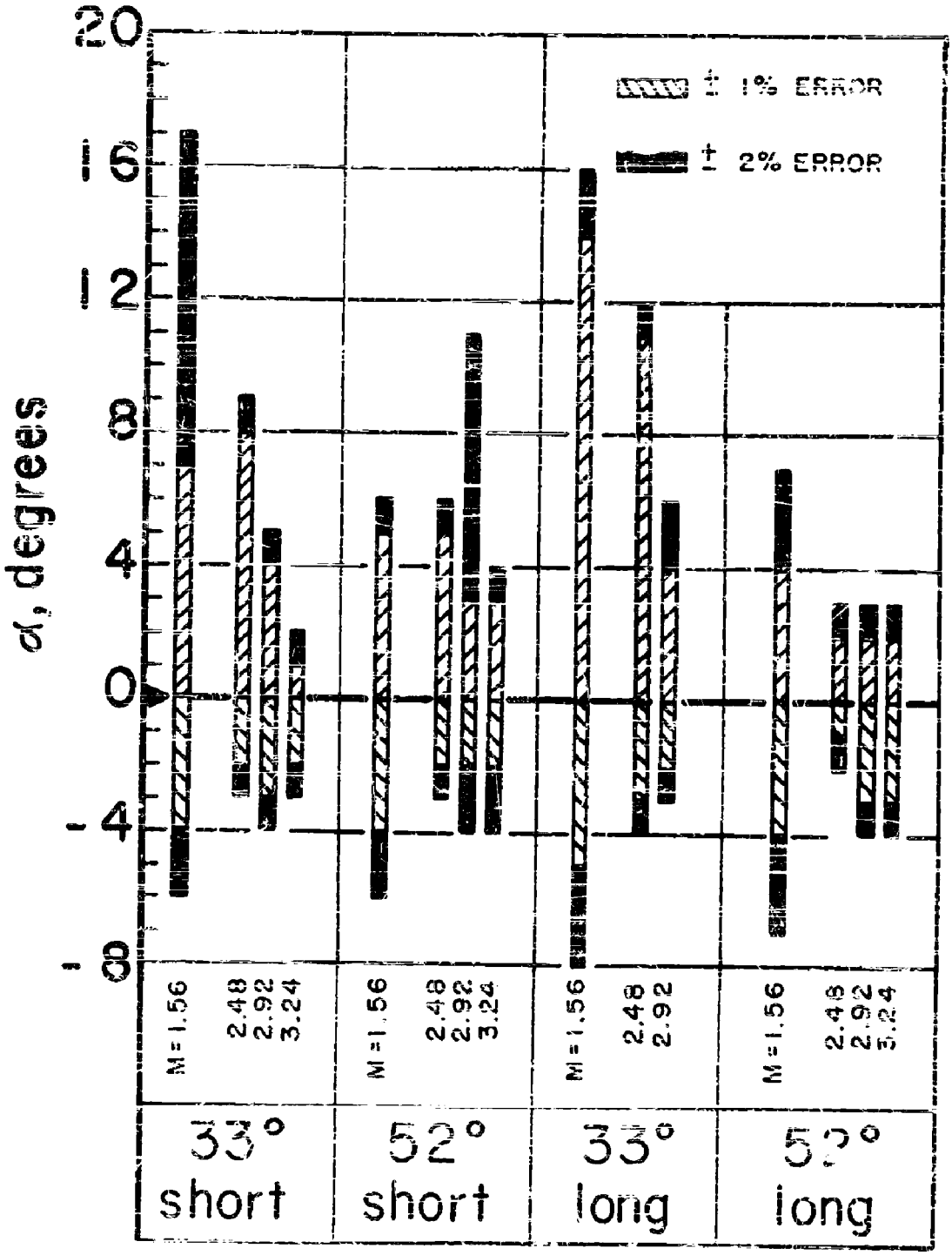

Fig. 7 Angle of Attack Range of Probes for Given Error Limit at Various M

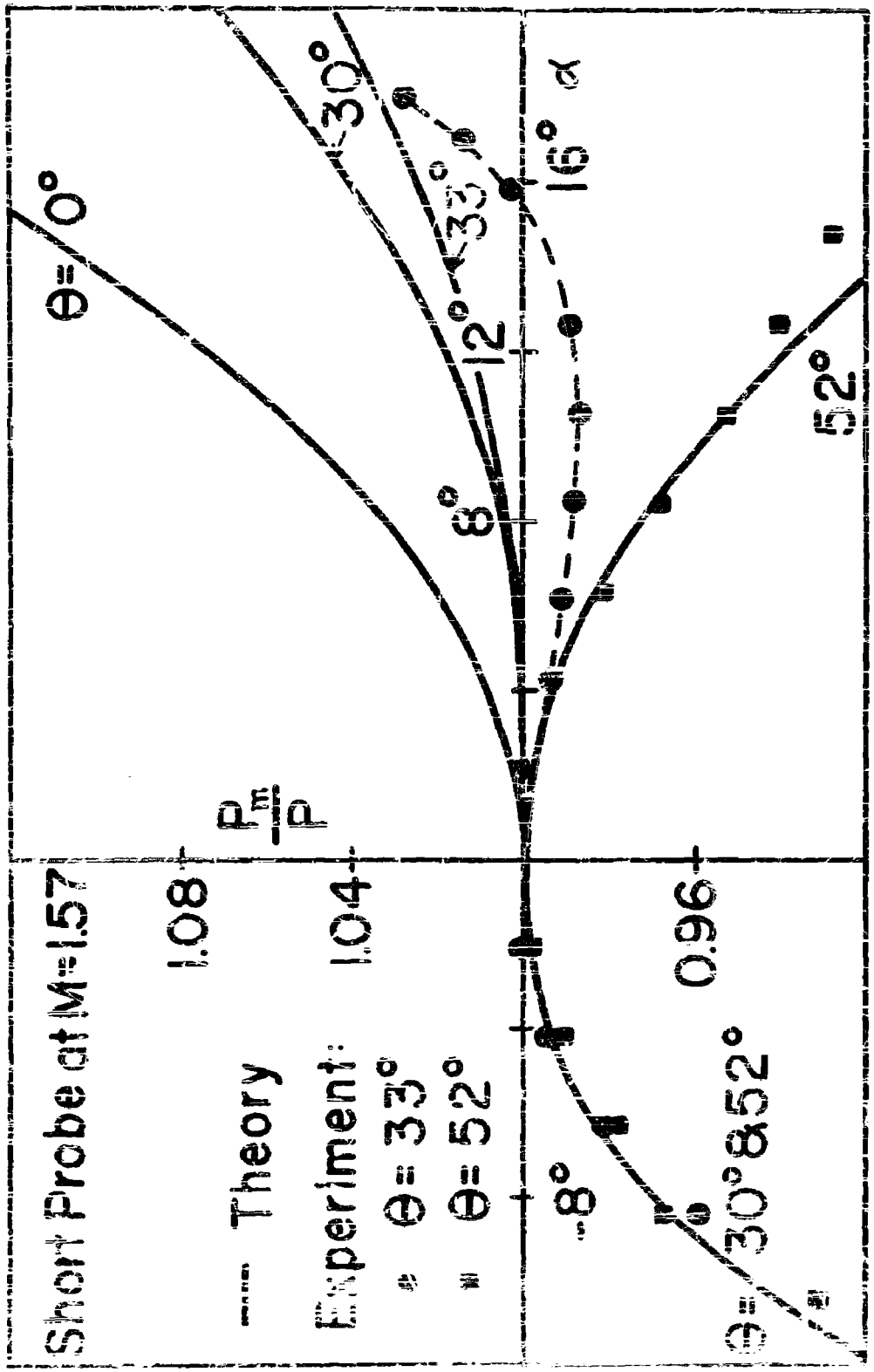

Fig. 8 Comparison of Pressure Distributions on Probes with Empirical Theory

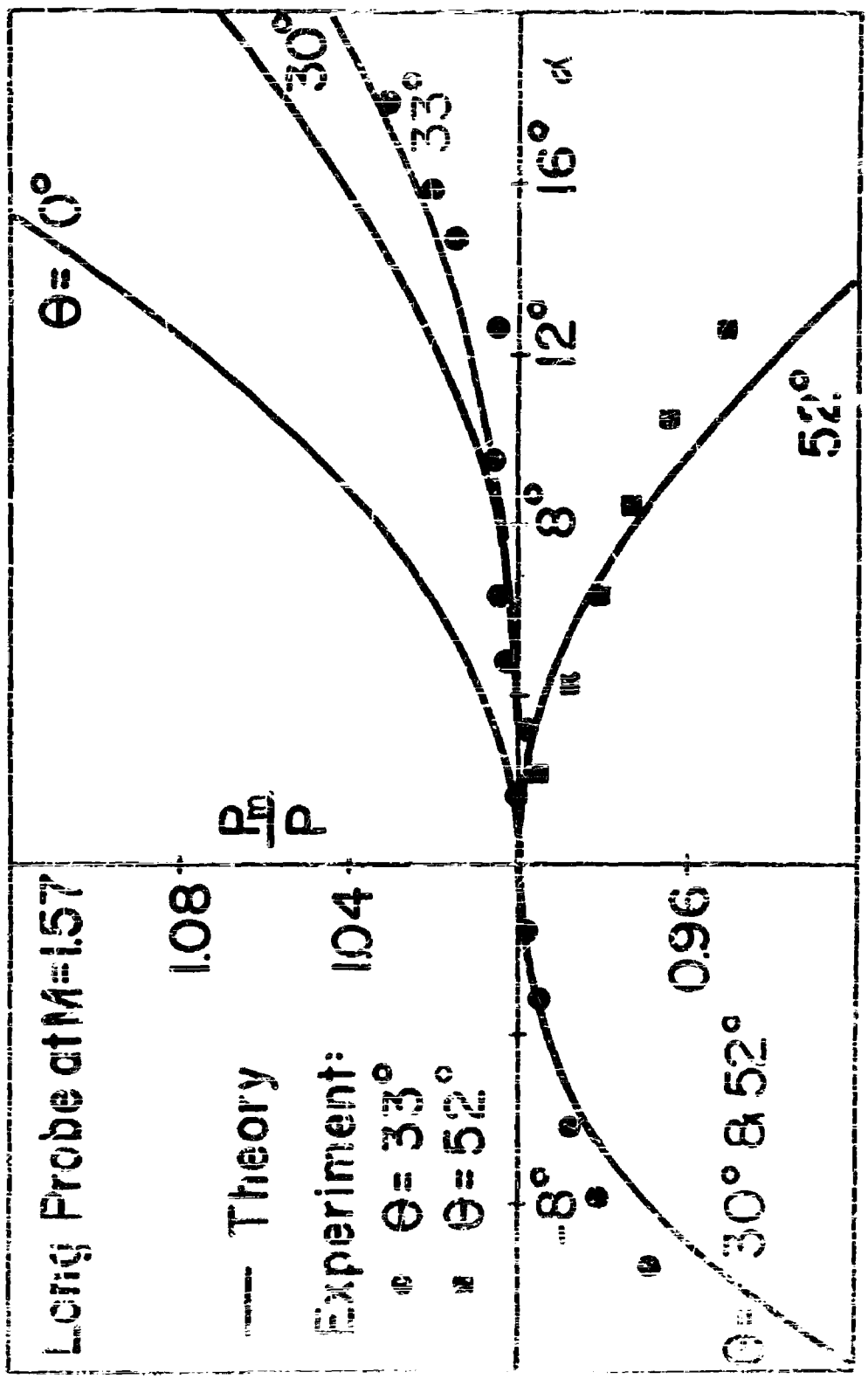

Fig. 9 Comparison of Pressure Distributions on Probes with Empirical Theory

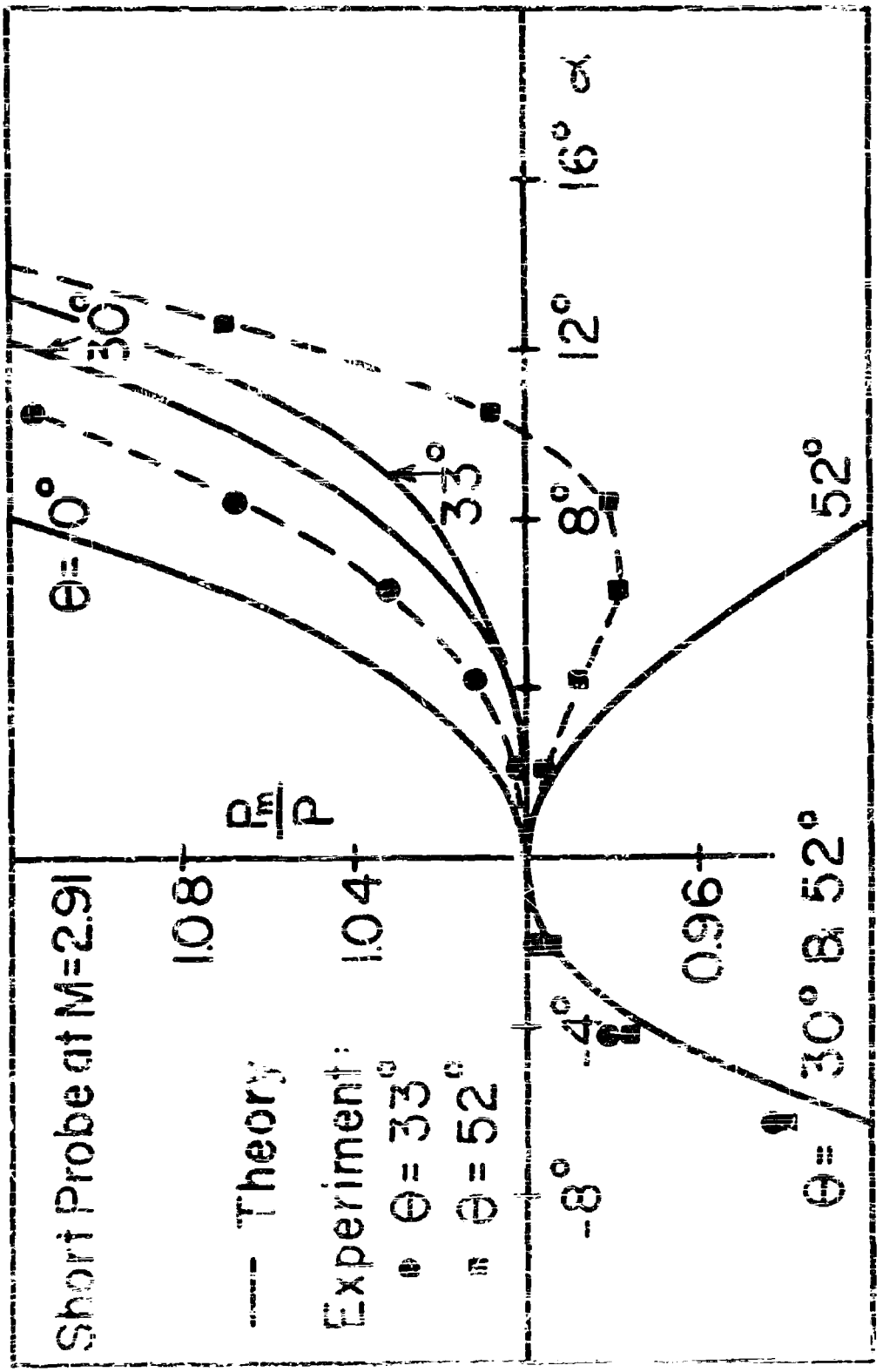

Fig. 10 Comparison of Pressure Distributions on Probes with Empirical Theory

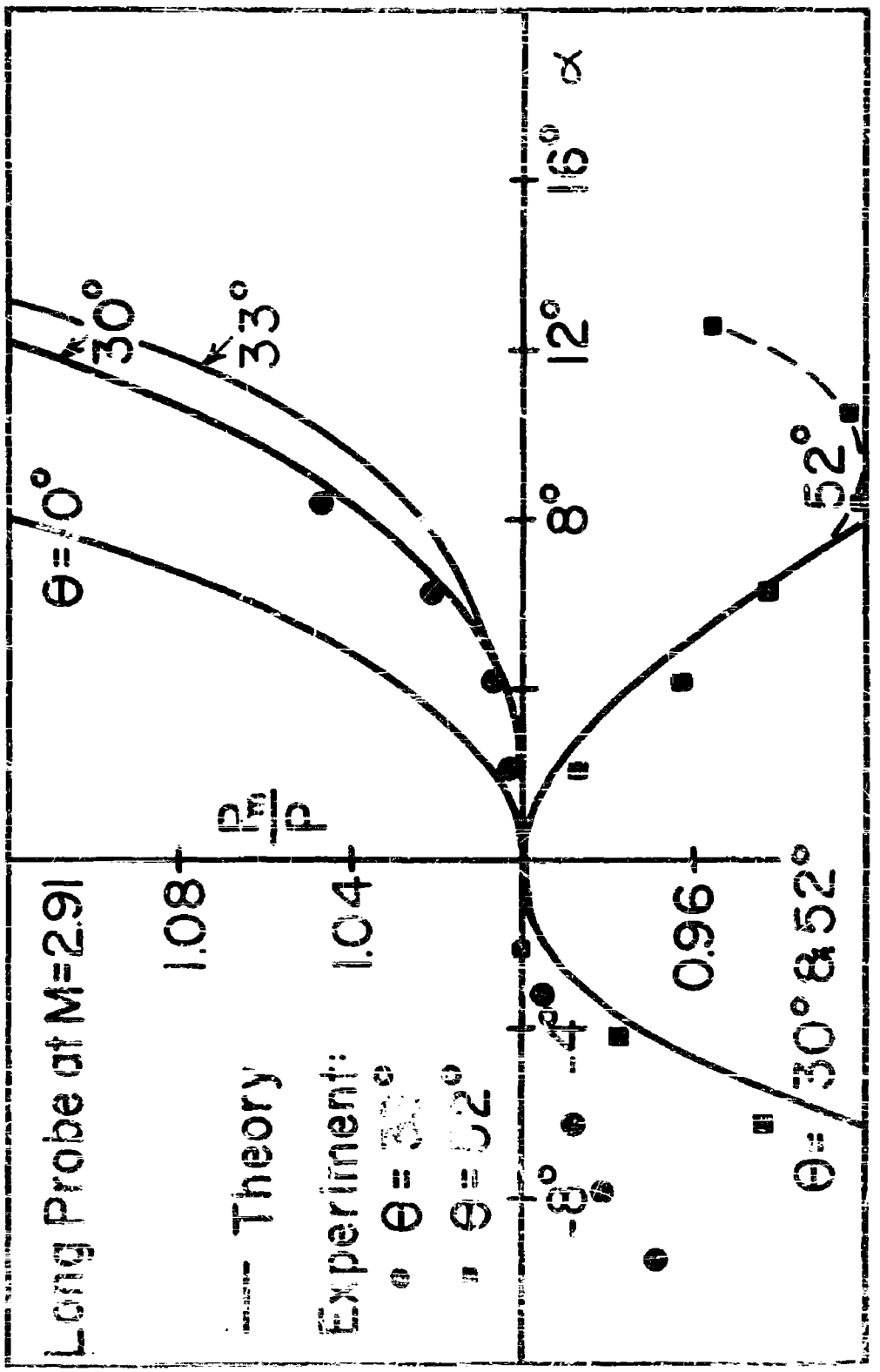

Fig. 11 Comparison of Pressure Distributions on Probes with Empirical Theory

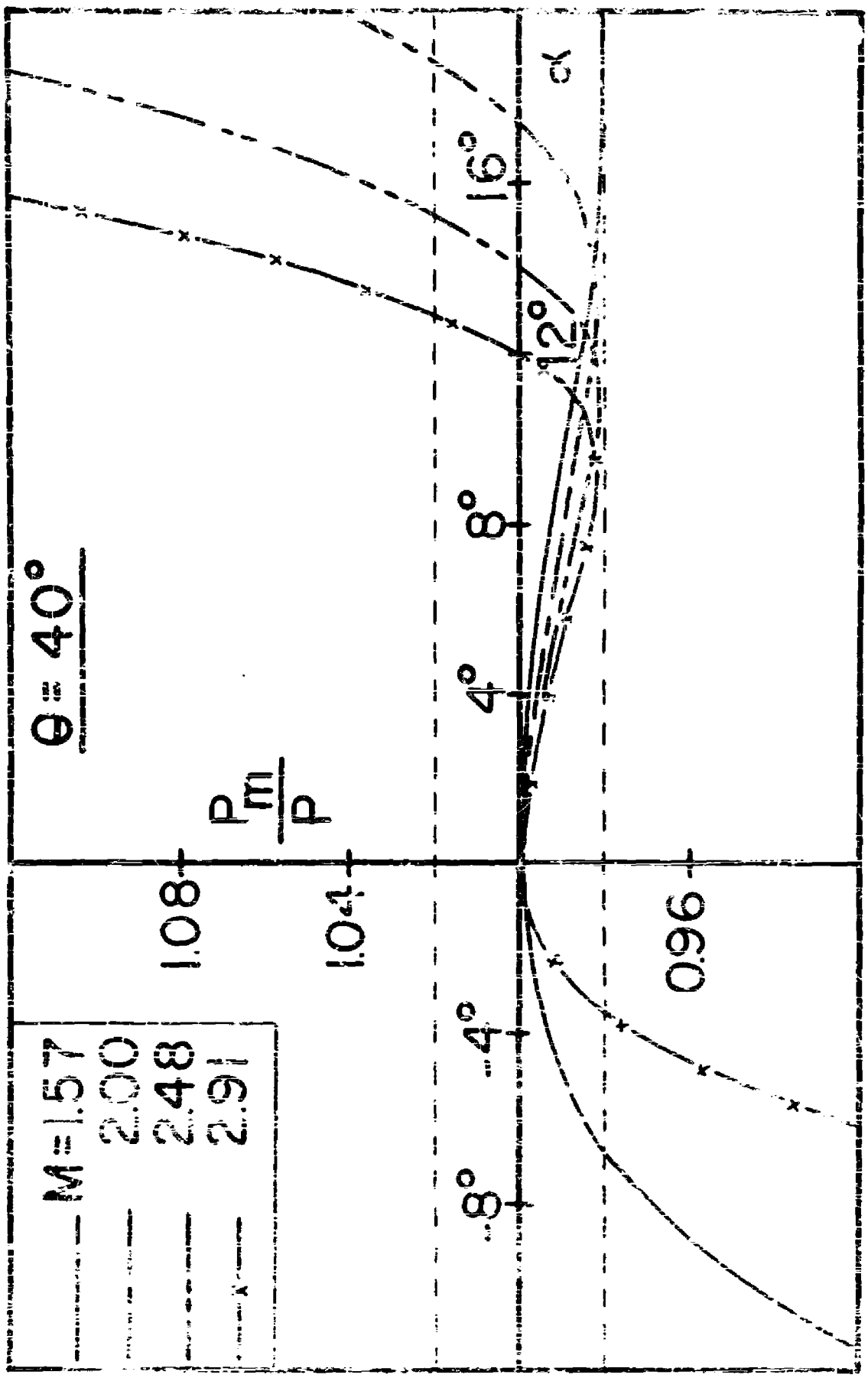

Fig. 12 Theoretical Pressure Distributions for θ = 40° Probes at Various M

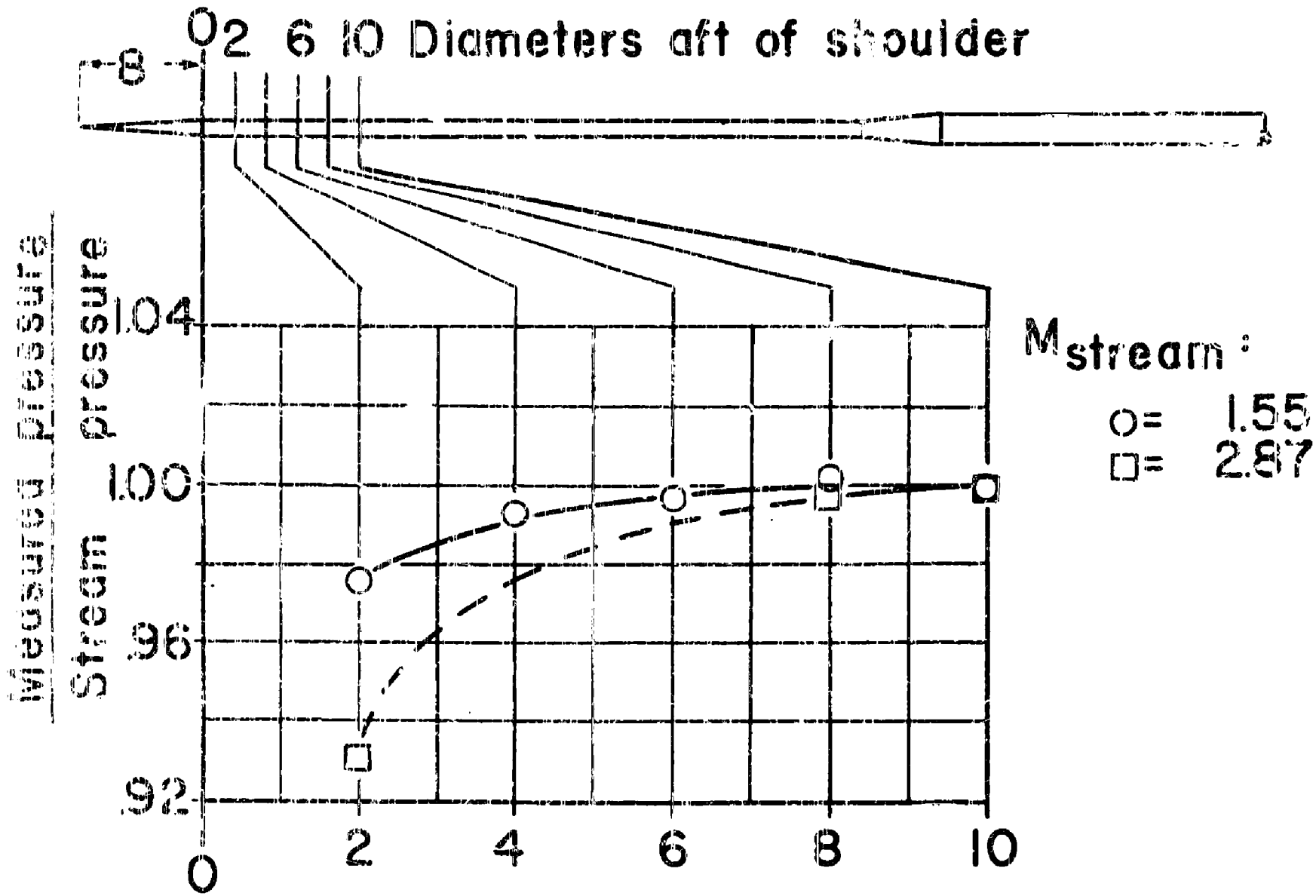

Fig. 13 Pressure at $\alpha = 0^\circ$ vs. Axial Location of Orifice

AEROBALLISTIC RESEARCH DEPARTMENT EXTERNAL DISTRIBUTION LIST

No. of Copies	
	Chief, Bureau of Ordnance Department of the Navy Washington 25, D. C.
1	Attn: Ree
1	Attn: Rexe
1	Attn: Re3d
2	Attn: Re6
3	Attn: Re9a
	Chief, Bureau of Aeronautics Department of the Navy Washington 25, D. C.
1	Attn: AER-TD-414
2	Attn: RS-7
	Commander U. S. Naval Ordnance Test Station Inyokern P.O. China Lake, California
2	Attn: Technical Library
1	Attn: Code 5003
	Commander U. S. Naval Air Missile Test Center Point Mugu, California
2	Attn: Technical Library
	Commanding Officer and Director David Taylor Model Basin Washington 7, D. C.
2	Attn: Hydrodynamics Laboratory
	Chief of Naval Research Library of Congress Washington 25, D. C.
2	Attn: Technical Info. Div.
	Office of Naval Research Department of the Navy Washington 25, D. C.
1	Attn: Code 438
2	Attn: Code 463
	Director Naval Research Laboratory Washington 25, D. C.
1	Attn: Code 2021
1	Attn: Code 2027

No. of Copies	
	Office, Chief of Ordnance Washington 25, D. C.
1	Attn: ORDTU
	Chief, AFSWP P.O. Box 2610 Washington 25, D. C.
1	Attn: Technical Library
	Commanding General Wright Air Development Center Wright-Patterson Air Force Base Dayton, Ohio
5	Attn: WCAPD
1	Attn: WCSD
2	Attn: WCSOR
2	Attn: WCRRN
1	Attn: WCACD
1	Attn: WCRRF
	Commanding General Aberdeen Proving Ground Aberdeen, Maryland
1	Attn: C. L. Poor
1	Attn: D. S. Dederick
	National Bureau of Standards Washington 25, D. C.
1	Attn: Nat'l Applied Math. Lab.
1	Attn: Librarian(Ord.Dev.Div.)
1	Attn: Chief, Mechanics Div.
	National Bureau of Standards Building 30, UCLA Campus 405 Hilgard Avenue Los Angeles 24, California
1	Attn: Librarian
	University of California 211 Mechanics Building Berkeley 4, California
1	Attn: Dr. R. G. Folsom
1	Attn: Mr. G. J. Maslach
1	Attn: Dr. S.A. Schaaf
	VIA: InMat

No. of Copies

California Institute of Technology
Pasadena 4, California
2 Attn: Librarian (Guggenheim Aero Lab)
1 Attn: Dr. H. T. Nagamatsu
1 Attn: Prof. M. S. Plesset
1 Attn: Prof. F. Goddard
1 Attn: Dr. Hans W. Liepmann
VIA: BuAero Representative

College of Engineering
Cornell University
Ithaca, New York
1 Attn: Prof. A. Kantrowitz
VIA: ONR

University of Illinois
202 E. E. R. L.
Urbana, Illinois
1 Attn: Prof A. H. Taub
VIA: InsMat

1 Director
Inst. for Fluid Dynamics and Applied Math
University of Maryland
College Park, Maryland
VIA: InsMat

University of Michigan
Willow Run Research Center
Ypsilanti, Michigan
1 Attn: L. R. Blasell
VIA: InsMat

University of Minnesota
Rosemount, Minnesota
1 Attn: J. Leonard Frame
1 Attn: Prof. N. Hall
VIA: Ass't InsMat

The Ohio State University
Columbus, Ohio
2 Attn: G. L. Von Eschen
VIA: Ass't InsMat

No. of Copies

Polytechnic Institute of Brooklyn
99 Livingston Street
Brooklyn 2, New York
1 Attn: Dr. Antonio Ferri
VIA: ONR

Princeton University
Princeton, New Jersey
1 Attn: Prof. S. Bogdonoff
1 Attn: Prof. L. Lees
VIA: ONR

Massachusetts Inst. of Technology
Cambridge 39, Massachusetts
2 Attn: Project Meteor
1 Attn: Guided Missiles Library

Applied Physics Laboratory
The Johns Hopkins University
8621 Georgia Avenue
Silver Spring, Maryland
1 Attn: Arthur G. Norris
VIA: NIO

1 Cornell Aeronautical Lab., Inc.
4455 Genesee Street
Buffalo 21, New York
VIA: BuAero Rep.

1 Defense Research Laboratory
University of Texas
Box 1, University Station
Austin, Texas
VIA: InsMat

Consolidated Vultee Aircraft Corp.
Daingerfield, Texas
1 Attn: J. E. Arnold
VIA: Dev. Contract Office

Douglas Aircraft Company, Inc.
3000 Ocean Park Boulevard
Santa Monica, California
1 Attn: Mr. E. F. Burton
VIA: BuAero Resident Rep.

No. of Copies

North American Aviation, Inc.
12214 Lakewood Boulevard
Downey, California
2 Attn: Aerophysics Library
VIA: BuAero Representative

United Aircraft Corporation
East Hartford 8, Connecticut
1 Attn: Robert C. Sale
VIA: BuAero Representative

National Advisory Committee for Aero
1724 F Street, Northwest
Washington 25, D. C.
5 Attn: E. B. Jackson

Ames Aeronautical Laboratory
Moffett Field, California
1 Attn: H. J. Allen
2 Attn: Dr. A. C. Charters

Langley Aeronautical Laboratory
Langley Field, Virginia
1 Attn: Theoretical Aerodynamics Div.
1 Attn: J. V. Becker
1 Attn: Dr. Adolf Buseman
1 Attn: Mr. C. H. McLellan
1 Attn: Mr. J. Stack

The Johns Hopkins University
Charles and 34th Streets
Baltimore 18, Maryland
1 Attn: Dr. Francis H. Clauser

1 Dr. Allen E. Puckett, Head
Missile Aerodynamics Department
Hughes Aircraft Company
Culver City, California

1 Dr. Gordon N. Patterson, Director
Institute of Aerophysics
University of Toronto
Toronto 5, Ontario, Canada
VIA: BuOrd (Adc)

No. of Copies

National Bureau of Standards
Aerodynamics Section
Washington 25, D. C.
1 Attn: Dr. G. B. Schubauer, Chief

Graduate School Aeronautical Engr.
Cornell University
Ithaca, New York
1 Attn: W. R. Sears, Director
VIA: ONR

1 Commander
U. S. Naval Proving Ground
Dahlgren, Virginia

Jet Propulsion Laboratory
4800 Oak Grove Drive
Pasadena, California
1 Attn: Dr. F. F. Wegener

Flight and Aerodynamics Lab.
Research Division
Ordnance Missile Laboratory
Redstone Arsenal
Huntsville, Alabama
1 Attn: J. L. Potter, Chief